

# Advantages of dual $CO_2$ & $O_2$ adsorption model for assessment of micropore development in biochar during two-stage gasification

**Korus, Agnieszka; Jagiello, Jacek; Jensen, Claus Dalsgaard; Sárossy, Zsuzsa; Ravenni, Giulia; Benedini, Lidia**

*Published in:*
Renewable Energy

*Link to article, DOI:*
10.1016/j.renene.2024.120293

*Publication date:*
2024

*Document Version*
Publisher's PDF, also known as Version of record

Renewable Energy 225 (2024) 120293

Contents lists available at ScienceDirect

Renewable Energy

journal homepage: www.elsevier.com/locate/renene

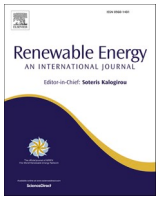

# Advantages of dual $CO_2$ & $O_2$ adsorption model for assessment of micropore development in biochar during two-stage gasification

Agnieszka Korus [a,*], Jacek Jagiello [b], Claus Dalsgaard Jensen [c], Zsuzsa Sárossy [c], Giulia Ravenni [c], Lidia Benedini [c]

[a] Department of Thermal Technology, Silesian University of Technology, Konarskiego 22, 44-100, Gliwice, Poland
[b] AGH University of Science and Technology, Faculty of Energy and Fuels, Department of Coal Chemistry and Environmental Sciences, Al. Mickiewicza 30, 30-059, Kraków, Poland
[c] Department of Chemical and Biochemical Engineering, Technical University of Denmark, Søltofts Plads 228A, Kgs.Lyngby, 2800, Denmark

ARTICLE INFO

Original content: Measurements and calculations for "Advantages of dual CO2 & O2 adsorption model for assessment of micropore development in biochar during two-stage gasification" (Original data)

*Keywords:*
Pore size distribution
Biochar
Micropores
Gasification

ABSTRACT

Residual biochar has the potential to replace commercial carbons even in highly specialised applications, presuming further advances in the engineered biochar production. Optimising biomass conversion requires dynamic feedback on the resultant char porosity, but investigation of pore size distribution (PSD) in pyrogenic carbons is challenging due to their extremely ultramicroporous nature. The most common probe molecule used in gas adsorption methods, $N_2$, is often unable to access the narrowest pores, while $CO_2$ can analyse only pores <10 Å.

We propose an approachable way to evaluate PSD of ultramicroporous carbons by simultaneously fitting the 2D-NLDFT (two-dimensional non-local density functional theory) kernels to the $CO_2$ and $O_2$ isotherms. Using $O_2$ as the probe molecule allowed collecting isotherms for the ultramicroporous pyrolytic char, for which a negligible adsorption of $N_2$ was observed. For the more activated, gasification chars, reaching equilibrium for $N_2$ adsorption took up to 8 h for some datapoints. $O_2$ adsorption was much faster, resulting in the total runtime more than two times shorter than for the $N_2$ tests.

By analysing chars from the semi-pilot scale gasifier, we confirmed the dependence of the char structure on the process parameters, but we also suspect a strong influence of the reactor design.

## 1. Introduction

Residual char from thermal conversion of biomass has found numerous applications, amongst other, as a green alternative to the commercial activated carbons [1–4]. An abundant and affordable material, its utilisation in, e.g., catalysis, filtration, or electrochemical processes has been intensely investigated [3,5–9].

Despite many advantages, working with biochar remains challenging due to its extreme heterogeneity [10]. Depending on the feedstock and the parameters of the conversion process, the final product might be hydrophobic of hydrophilic, have more acidic or basic active sites [11]. Carbon planes arrangement and aromaticity, and the extent of pore development and surface area might also differ significantly [12–15].

Many factors influence biomass carbonization – even the well-recognized trends in char formation may not be sufficient to successfully predict the properties of the final product [10,11]. The lack of consensus on how to evaluate surface area and pore distribution, and the discrepancies between the results obtained with different methods, leads to a further disarray [16].

Finding the best approach to pore assessment should account for the properties of the carbon lattice (e.g., surface energetical heterogeneity) as well as the range of pore sizes that dominate the distribution. Following IUPAC report [17], the main classes of pores that can be analysed with gas adsorption methods include ultramicropores (<7 Å), supermicropores (7–20 Å), and mesopores (20–500 Å). The narrowest pores are the most challenging when selecting the appropriate probe molecule for the adsorption analysis. Access to these structures is limited not only by the kinetic diameter of the probe molecule, but also by its interactions with the carbon surface, and the connectivity of the pores, which might further hinder diffusion into the smallest cavities [16,18,19].

Pyrogenic carbons, such as chars form biomass pyrolysis or gasification, are extremely microporous materials [18,20]. Even gasification,

* Corresponding author.
*E-mail address:* agnieszka.korus@polsl.pl (A. Korus).

https://doi.org/10.1016/j.renene.2024.120293
Received 2 January 2024; Received in revised form 28 February 2024; Accepted 7 March 2024
Available online 8 March 2024

**Abbreviations and symbols**

| | |
|---|---|
| 2D-NLDFT | Two-dimensional non-local density functional theory |
| DTU | Technical University of Denmark |
| IUPAC | International Union of Pure and Applied Chemistry |
| PSD | Pore size distribution |
| SAIEUS | Solution of Adsorption Integral Equation Using Splines |
| SI | Supplementary Information |
| $w_{min}$ | Lower pore width limit, Å |
| V | Total pore volume, $cm^3/g$ |
| S | Total surface area, $m^2/g$ |

which develops some mesopores in the char, does not expand all the pores, maintaining the dominating contribution of ultramicropores in the total surface area [18]. Hence, the main stress during pyrogenic carbon structure investigation should be placed on the suitable probe molecules selection.

Adsorption of $CO_2$ at 273 K is particularly convenient for the analysis of carbon molecular sieves and microporous carbons [21,22], as it easily enters ultramicropores. However, it was determined that this probe molecule can be used to measure pores up to 10 Å [19], thus it is typically used in tandem with another compound to obtain complete pore size distribution in the range of 3.6–500 Å. $N_2$ is usually used as the second molecule, its isotherm fitted simultaneously into a dual model. However, with the restricted access to the pores, $N_2$ measurement at low partial pressure is extremely time-consuming and often inaccurate. On the other hand, using $O_2$ at cryogenic conditions has recently gained interest due to a much lower quadruple moment, which speeds up the analysis [20,23,24]. So far, the use of $O_2$ has been studied to analyse carbon sieves and carbon blacks [25], or carbons synthesised from organic precursors such as phloroglucinol/glyoxylic acid or glucose [24]. Recently, Blankenship et al. [20] examined biomass-derived carbons from hydrothermal carbonization of sawdust. For the pore size distribution (PSD) calculations in these works, $O_2$ was used as a standalone gas [24] or has been coupled with the $H_2$ adsorption isotherm to better characterize ultramicropores [20,25]. Although $H_2$ has smaller diameter and quadrupole moment than $CO_2$, its high flammability and permeability might constrain hydrogen use in the less advanced gas adsorption analysers.

In this work, we examine the combination of widely used $CO_2$ and yet less conventional $O_2$ probe molecules. We simultaneously fitted dual two-dimensional non-local density functional theory (2D-NLDFT) models dedicated to carbons with heterogenous surface [26] to the adsorption isotherms measured with these gases. Such approach is aimed at convenient characterisation of residual biochar from industrial processes.

Diversity of biochar properties requires their characterisation with each modification or scale-up of the biomass conversion process. Hence, a consistent, time-efficient, and accessible method for pore size distribution for biochar comparison would be desirable.

To assess the proposed $CO_2$ & $O_2$ isotherms combination and its applicability to chars with different pore accessibility, we examined chars sampled from the semi-pilot two-stage gasifier developed at the Technical University of Denmark (DTU). This reactor comprises two units – the first produces pyrolytic char, which is subsequently activated in the second unit. Char was collected after each of these steps, giving a set of two samples (pyrolytic and gasification char) for each test run. The char sets from four tests, differing in gasifying agent and temperature, were investigated.

This way, we were able to examine extremely ultramicroporous chars from pyrolysis, as well as the more open-structured gasification chars. With these versatile samples we were able to validate the applicability of the $CO_2$ & $O_2$ dual model for pyrogenic carbons evaluation.

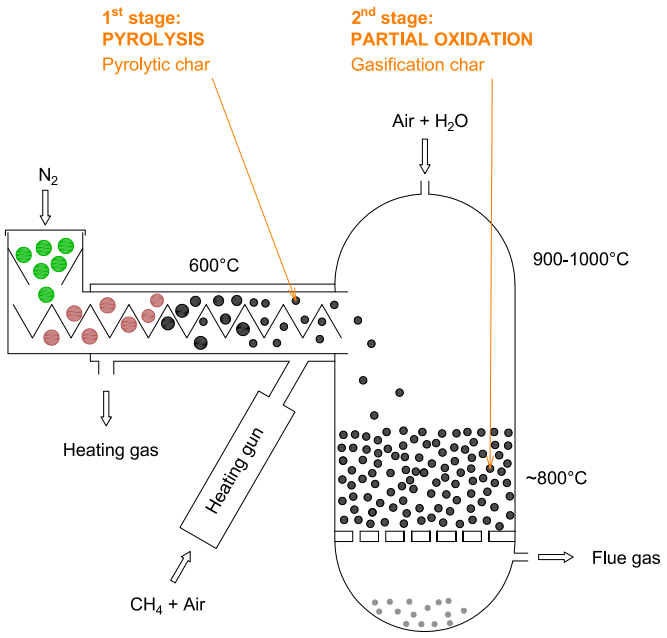


**Fig. 1.** Schematic of the two-stage gasifier at DTU (based on [27]).

Meanwhile, following the fate of the char between the steps of pyrolysis and gasification provided an insight into the transformation of this material during interactions with the gasifying agents (steam and $CO_2$). Applying different gasification conditions allowed evaluating the sensitivity of the char structure development to the selected process parameters and highlighted the significance of the reactor's design.

## 2. Experimental

### 2.1. Char preparation and characterization

Residual char obtained from straw pellet gasification was used to investigate pore development assessed with the gas adsorption method using different probe molecules. The straw conversion was performed in the semi-pilot-scale two-stage gasifier with 50 kW thermal output (Fig. 1). In this reactor, developed at DTU, biomass devolatilization (1st stage) is separated from the following volatiles-char interactions (2nd stage). The first process occurs in the screw pyrolysis unit, externally heated with hot gases to 600 °C. Here, under $N_2$ flow, volatiles and gases are released from the biomass, leaving solid residue, i.e., the pyrolytic char. All the pyrolysis products are then directed into the downdraft gasifier. Air, and optionally steam, are fed from the top of the gasifier, where they partially oxidize the volatile compounds. The temperature in the gasifier (900, 950, or 1000 °C) is controlled by the air supply adjustment. The pyrolytic char, propelled by the pyrolysis unit's screw, falls down this high-temperature zone to the bottom of the gasifier, where it accumulates as a fixed bed (note that the bed temperature is

**Table 1**
Parameters of gasification experiments and abbreviations assigned to the char samples.

| Exp. | Gasification temperature | Steam (kg water/kg feedstock) | Pyrolytic char [a)] | Gasification char |
|---|---|---|---|---|
| 1 | 900 °C | none | P900 | G900 |
| 2 | 950 °C | none | P950 | G950 |
| 3 | 1000 °C | none | P1000 | G1000 |
| 4 | 1000 °C | 1/5 | P1000H2O | G1000H2O |

[a)] Note that for the "P" chars the same condition-related abbreviation as for the "G" chars was used although the gasification conditions did not influence the "P" chars, as they were sampled prior to the gasification stage.

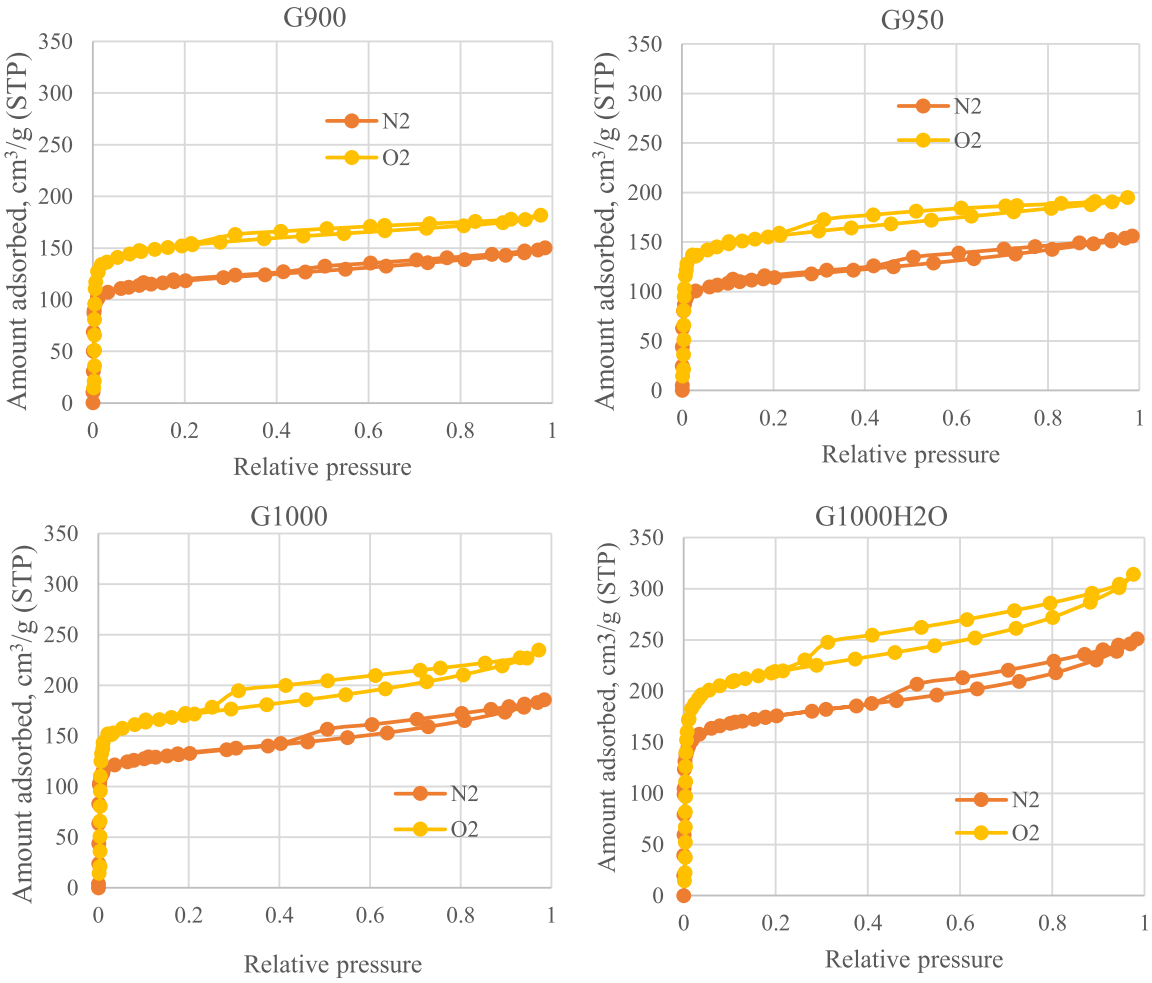


**Fig. 2.** Isotherms of $N_2$ and $O_2$ adsorption on the gasification chars from four experimental runs with different gasification conditions.

lower than the gases above it, around 800 °C). The partially oxidized volatiles and gases travel through this bed on their way out, thus interacting with the char. These interactions involve both char oxidation with the gasifying agents, and coke deposition from the reforming volatiles. However, the overall balance leads to carbon consumption, which increases the porosity of the carbon, similar to the thermal activation methods for activated carbon production. Thus, the gasification char, collected from the gasifier, has an increased porosity compared with the char sampled at the end of the pyrolyzing unit, i.e., the pyrolytic char.

To investigate the magnitude of pore formation, four gasification conditions were tested. From each experiment, the samples of pyrolytic and gasification char were collected, as listed in Table 1. It should be noted that only the gasification step was altered, and the pyrolysis parameters were constant. All four pyrolytic char samples were formed under similar conditions; thus, they can be considered quadruplicates of the same material, collected from different batches of the pyrolysis process.

### 2.2. Gas adsorption measurements

The analysis of the collected chars was performed with the gas adsorption method using a Micromeritics TriStar II 3020 (Micromeritics) analyser with the krypton option (i.e., featured with additional transducer for measuring pressures <10 mm Hg, and a high-vacuum pump). Three different probe molecules were used for gas adsorption tests – $N_2$ isotherm at 77 K, $O_2$ isotherm at 77 K, and $CO_2$ isotherm at 273 K were collected for each sample. The $CO_2$ adsorption was measured up to 1 atm absolute pressure, which corresponds to $CO_2$ relative pressure of 0.03, and accounts for pores up to 10 Å. The $N_2$ and $O_2$ isotherms were collected for the relative pressure range of $10^{-3}$ to 0.98. For the comparison, two sample were additionally analysed with NOVAtouch LX2 (Quantachrome), which is dedicated to the $N_2$ adsorption measurements in the same pressure range as TriStar. Prior to the analyses, all samples were degassed for 24 h at 200 °C under vacuum.

Two types of chars were analysed; for each type, the analysis parameters were adjusted to account for their structural difference. The pyrolytic chars, due to high ultamicroporosity, have limited accessibility for some probe molecules. For the gasification chars, where there was no constriction in pore penetration, an equilibration interval of 40 s was applied for the data points measured at relative pressures <0.01. Long equilibration times, while providing high accuracy, in the case of the very narrow pores, can prolong the measurements, making the analysis difficult to complete in a reasonable time. Thus, to collect the isotherms for the pyrolytic chars, more lenient criteria for equilibrium state determination were tested. For the $N_2$ adsorption on pyrolytic chars, both 15 and 40 s equilibration intervals resulted in short analysis time, and a negligible quantity of $N_2$ was adsorbed, proving the pores were inaccessible. When 15 s equilibration interval was applied during $O_2$ analysis, no equilibrium state could be reached within 48 h, even for one datapoint, suggesting that the pores were partially accessible for this molecule, yet the criteria were too severe to enable measurement of the isotherm in a timely manner. However, the measurement proved possible when 5 s equilibration interval was used, resulting in the well-defined $O_2$ adsorption isotherm.

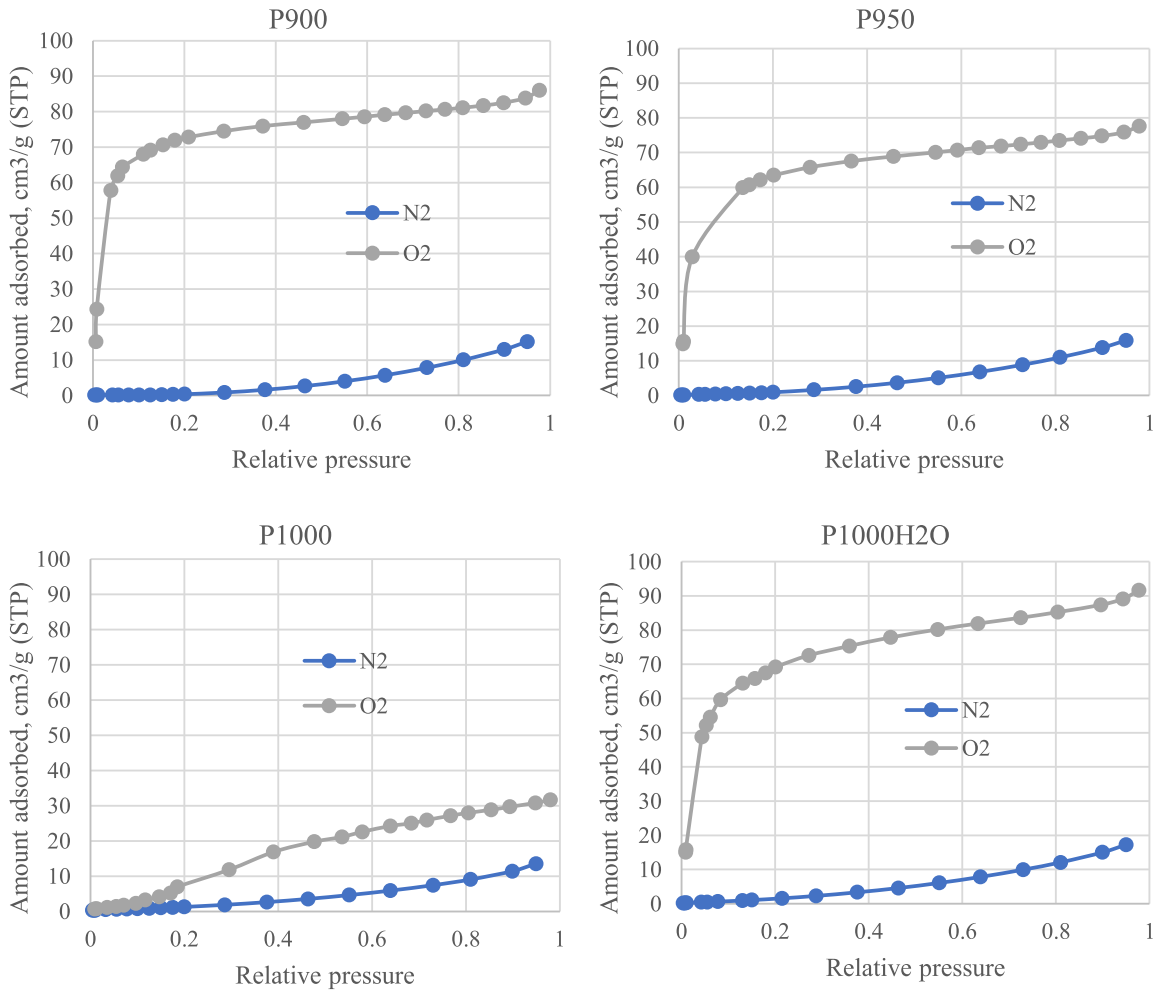


**Fig. 3.** Isotherms of $N_2$ and $O_2$ adsorption the pyrolytic chars from four experimental runs (all prepared under the same conditions).

Uniform conditions, with 20 s equilibration interval, were applied for pyrolytic and gasification char analysis with $CO_2$, as this molecule accessed the pores without any constrictions.

### 2.3. Pore size distribution calculations

Pore size distribution (PSD) was calculated with SAIEUS software. This numerical algorithm allows simultaneously fitting a few probe molecules' kernels to the respective measured isotherms. The $CO_2$ & $N_2$ as well as $CO_2$ & $O_2$ combinations were compared in this paper. Since negligible $N_2$ adsorption was measured for the pyrolytic chars, the $CO_2$ isotherm only was used instead of $CO_2$ & $N_2$ for these samples. The $O_2$ and $N_2$ single models, as well as a dual $O_2$ & $N_2$ and triple $CO_2$ & $O_2$ & $N_2$ fittings were also tested for the selected samples to verify the coherence between the obtained PSDs.

The PSD calculations used the 2D-NLDFT models dedicated to the carbons with heterogeneous surfaces and slit-shaped pores developed by Jagiello and Olivier [26,28]. The SAIEUS algorithm employs a regularization method combined with non-negativity constraints [29], where the lambda parameter is used to optimize the balance between the fitting error and the roughness of PSD plot. For consistency, the lambda parameter adjustment was done globally; it was set to a fixed value of 4.5 for all the samples, to ensure unbiased PSD results (with the except of dual $O_2$ & $N_2$ fittings that required lambda of 5 due to high roughness).

The PSDs were calculated for the pore width range of 3.6–500 Å. However, for the dual $CO_2$ & $O_2$ fitting to the isotherms measured for the pyrolytic chars, the lower pore width limit $w_{min}$ of the $O_2$ kernel was increased to 5 Å, so that the smallest of the pyrolytic char pores were determined solely from the $CO_2$ isotherm, which is more accurately measured. Increasing the $w_{min}$ for the kernels of probe molecules that have constrained access to the carbon ultramicropores is a procedure recommended to improve quality of the fit [30].

## 3. Results and discussion

### 3.1. $O_2$ and $N_2$ isotherms

The $N_2$ and $O_2$ adsorption isotherms collected for the gasification chars are presented in Fig. 2. As expected, the more severe gasification conditions, i.e., higher temperature and addition of steam, enhanced porosity development, observed as the increasing gas adsorption for G900 < G950 < G1000 < G1000H2O chars. For all samples, both $N_2$ and $O_2$ measurements gave isotherms typical for micro-mesoporous biochar materials – i.e. the combination of type I and II isotherms with H4 hysteresis loop [31]. Compared with $N_2$, a higher $O_2$ uptake by all samples was observed, yet it was likely the result of the higher density of this probe molecule – both isotherms gave consistent PSDs and similar pore volumes. The main advantage of $O_2$ was the shorter time required to reach equilibrium for the less activated char measurements, cutting down the analysis time from approx. 30 to 13 h. Time intervals between the measured points are provided in Supplementary Information (SI) S1. Quicker analysis with $O_2$ was also reported by Blankenship et al. [20]

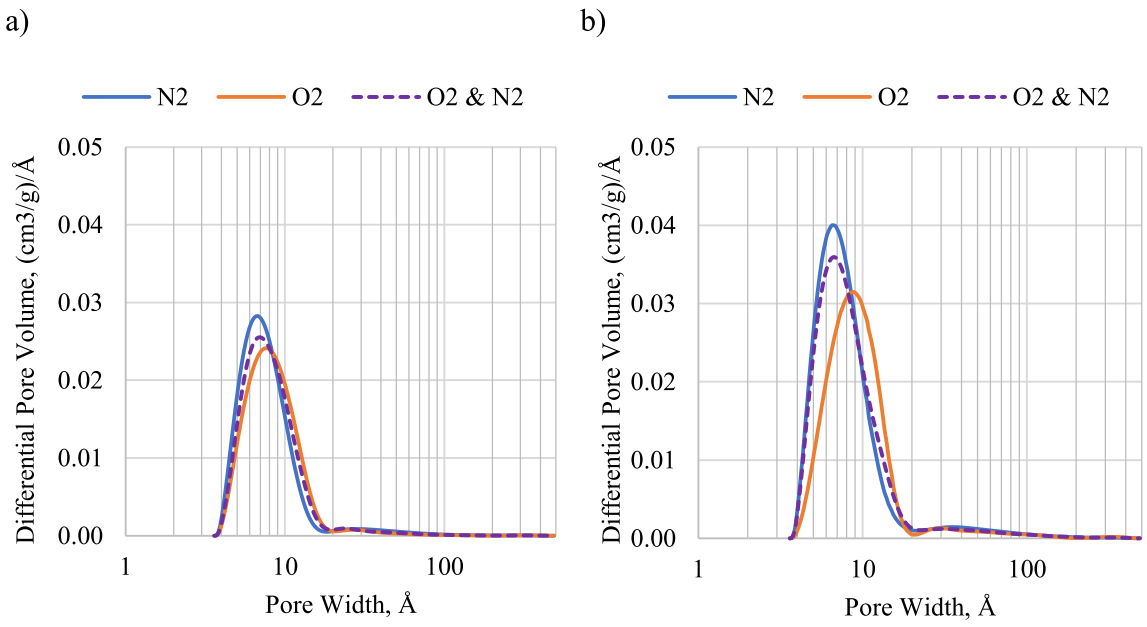


**Fig. 4.** PSD in a) G900 and b) G1000H2O calculated from the $N_2$ and $O_2$ only, and the simultaneous fit to both isotherms.

who advocate using this gas for microporous carbon analysis.

Interesting phenomenon was observed during pyrolytic biochar analysis. All examined samples had the same thermal history (pyrolysis at 600 °C), resulting in the replicable gas adsorption results (Fig. 3). In all cases $N_2$ failed to access the micropores, giving isotherms without the initial vertical increase (meaning no accessible micropores) and with the insignificant overall adsorption. Similar results were obtained with another instrument with the comparable specification, i.e., $p/p_0$ range of $10^{-3}$-1 (SI S2). However, $O_2$ as a probe molecule successfully entered the pores in three samples; only for P1000 the adsorption was still poor. These findings suggest that the analysis of the extremely microporous carbons can be achieved without the low pressure ($p/p_0 < 10^{-3}$) measurements by simply changing the probe molecule from $N_2$ to $O_2$.

### 3.2. Fitting NLDFT model to single and multiple isotherms

The investigation on using $O_2$ as a probe molecule was initiated by calculating pore size distributions (PSDs) of the gasification chars based on the $N_2$ and $O_2$ isotherms, as the model fitting was possible for both isotherms collected for these samples. The comparison of the obtained distributions is presented in Fig. 4. Additionally, a simultaneous fit to both isotherms was made to verify the consistency of the two models.

In general, $O_2$ gave a slightly wider distribution, especially for the more activated char (G1000H2O). The simultaneous fitting resulted in the PSD averaging the two single-isotherm cases. Importantly, a satisfactory fit (SI S3) was obtained for the dual approach, suggesting compatibility between the results obtained with these two probe

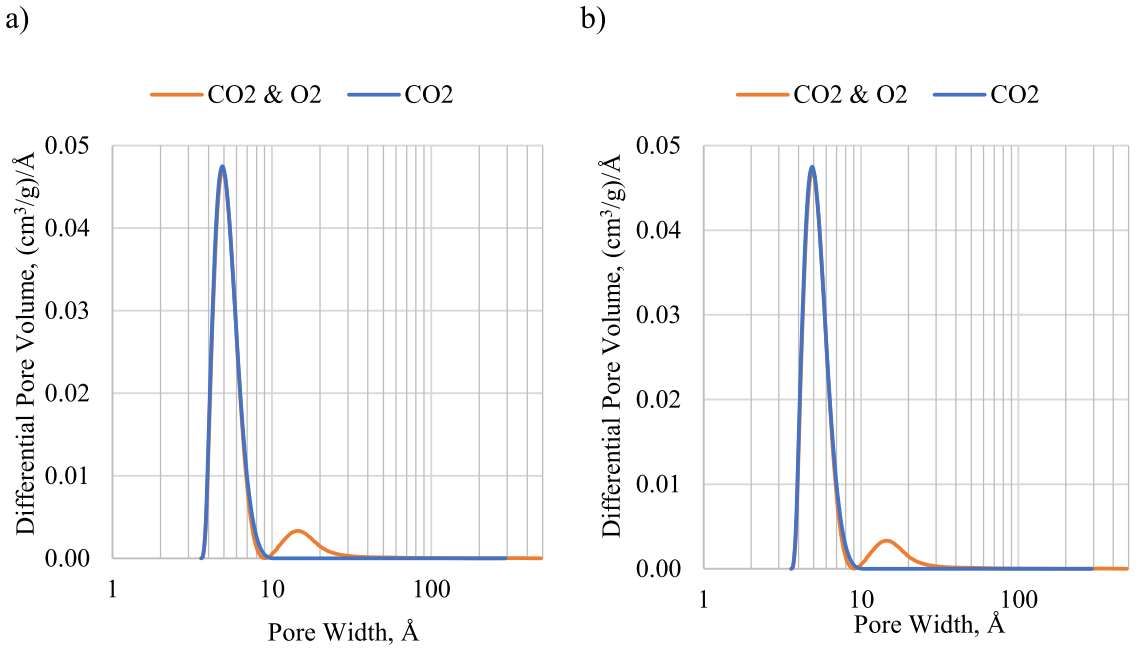


**Fig. 5.** PSD in a) P900 and b) P1000H2O for the $CO_2$ isotherm only and the dual $CO_2$&$O_2$ fit.

**Table 2**
Total surface area (S) and total pore volume (V) of the pyrolytic chars calculated with the single and dual 2D-NLDFT models.

| | $N_2$ | | $O_2$ | | $CO_2$ | | $CO_2$ & $O_2$ | |
|---|---|---|---|---|---|---|---|---|
| | V, $cm^3/g$ | S, $m^2/g$ | V, $cm^3/g$ | S, $m^2/g$ | V, $cm^3/g$ | S, $m^2/g$ | V, $cm^3/g$ | S, $m^2/g$ |
| P900 | 0.02 | 5.9 | 0.10 | 177 | 0.10 | 388 | 0.14 | 416 |
| P950 | 0.02 | 6.7 | 0.09 | 121 | 0.10 | 366 | 0.13 | 382 |
| P1000 | 0.02 | 5.9 | 0.04 | 18 | 0.08 | 294 | 0.08 | 249 |
| P1000H2O | 0.03 | 7.6 | 0.10 | 140 | 0.11 | 369 | 0.14 | 371 |

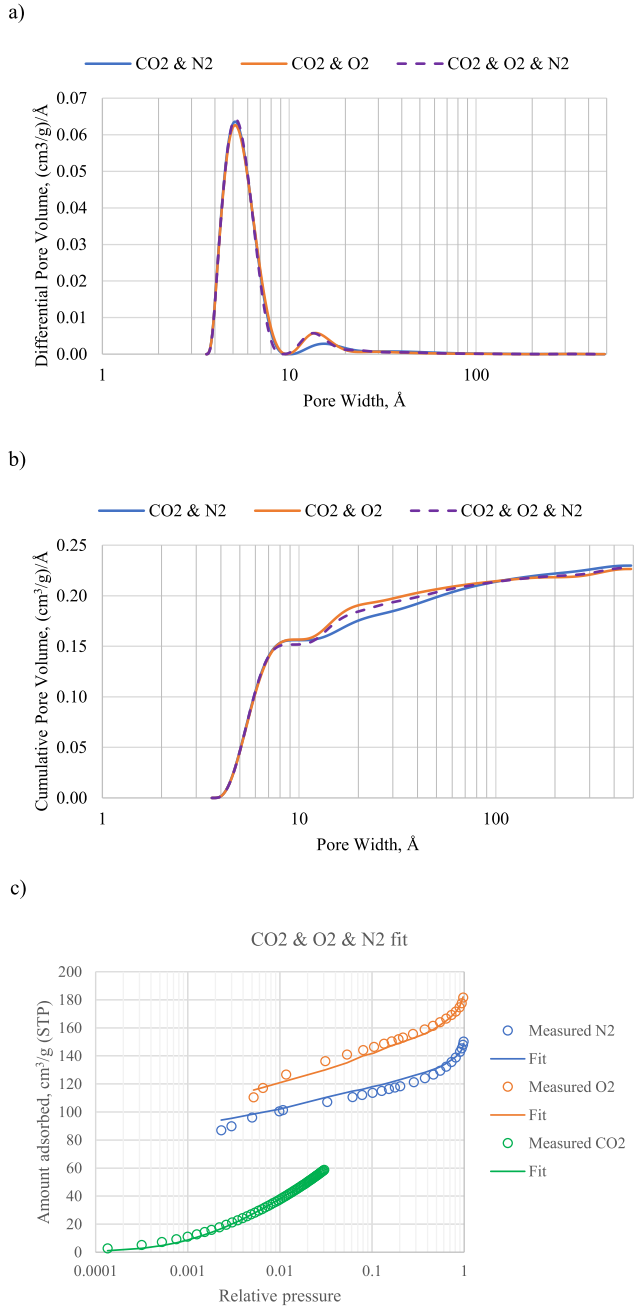


**Fig. 6.** Comparison of the PSDs (a) and cumulative pore volumes (b) of G900 char calculated with multiple-isotherm models, and the simultaneous fit to three measured isotherms (c).

**Table 3**
Total surface area (S) and total pore volume (V) of gasification chars obtained from the dual 2D-NLDFT models and the specific surface area calculated from $N_2$ isotherm with the BET method.

| | $CO_2$ & $N_2$ | | $CO_2$ & $O_2$ | | BET $N_2$ |
|---|---|---|---|---|---|
| | V, $cm^3/g$ | S, $m^2/g$ | V, $cm^3/g$ | S, $m^2/g$ | S, $m^2/g$ |
| G900 | 0.230 | 617 | 0.227 | 631 | 456 |
| G950 | 0.240 | 614 | 0.242 | 641 | 433 |
| G1000 | 0.283 | 673 | 0.283 | 686 | 515 |
| G1000H2O | 0.374 | 764 | 0.371 | 767 | 675 |

molecules, when the gasification chars, with more accessible pores, were examined.

The pyrolytic char had no contact with the reactive gases. Thus, it is highly microporous and $N_2$ was unable to enter the investigated material. On the other hand, it was possible to obtain $O_2$ isotherms for three out of four samples. Meanwhile, the agreement between $N_2$ and $O_2$-based PSDs obtained for the gasification chars suggest that $O_2$ is a suitable probe molecule for analysis of the pyrogenic types of carbons.

Biochar, both pristine (pyrolytic) and activated (gasification), possesses large share of ultramicropores. Thus, incorporating in the calculations the $CO_2$ isotherm, which allows for the analysis of the pores in the range of 3.6–10 Å, is highly important, if the full overview of the pore sizes is sought. Typically, the simultaneous fit to $CO_2$ and $N_2$ isotherms is applied. Since for the investigated pyrolytic chars $N_2$ isotherm could not be used, only the dual fit of $CO_2$ and $O_2$ isotherms was performed. Moreover, the PSD based on the $CO_2$ only was also calculated; the examples of both approaches are presented in Fig. 5. Good agreement between the results of single and dual gas analysis was observed – the main peak at 5 Å was consistent in both PSDs. The inclusion of the $O_2$ isotherm resulted in the additional small peak of supermicropores with the size of approx. 15 Å.

Interestingly, an unforced agreement between the modelled and the physically justified pore size range was observed for the single fit to the $CO_2$ isotherm only. Despite the full set of theoretical isotherms used for the fitting, obtained PSDs were in the range of pore widths physically possible to be measured with $CO_2$ adsorption at 273 K (<10 Å).

The pyrolytic char was highly ultramicroporous, thus the $CO_2$ measurement was crucial for the thorough evaluation of its porosity. Total pore volumes and surface areas of pyrolytic chars calculated using different isotherm combinations are presented in Table 2. As the measured $N_2$ adsorption was negligible, porosity of the pyrolytic chars calculated with $N_2$ isotherm was marginally small. On the other hand, in most cases, $O_2$ was able to penetrate some supermicropores, suggesting surface area exceeding 100 $m^2/g$. Furthermore, the $CO_2$ measurement, aimed at ultramicropores detection, revealed a significant surface area attributed to these pores. Finally, the simultaneous fitting to the $CO_2$ and $O_2$ isotherms joined the ultra and supermicropore contributions, providing the most detailed assessment of the PSD.

Most studies on the pyrolytic char are based on $N_2$ isotherms and thus report it as non-porous. Investigating this material with different probe molecules showed that it possesses a well-developed, though highly microporous, structure. Such narrow pores play an important role in some phenomena, e.g., metal intercalation [24,32]. Thus, an extended analysis of pyrolytic chars might help to reveal their potential in numerous new applications.

The gasification chars were evaluated with the dual models, using either $CO_2$ & $N_2$ or $CO_2$ & $O_2$ adsorption isotherms. The PSDs and model fittings for all gasification samples are provided in the SI S5, while the incremental and cumulative pore volumes of the G900 are presented in Fig. 6, as an example. Additionally, the simultaneous calculation for all three probe molecules were made and it showed consistent results and good fit to the experimental data (Fig. 6c).

Similar to the pyrolytic char, in the gasification char ultramicropores were the dominating structure. The presence of the larger micropores, i.

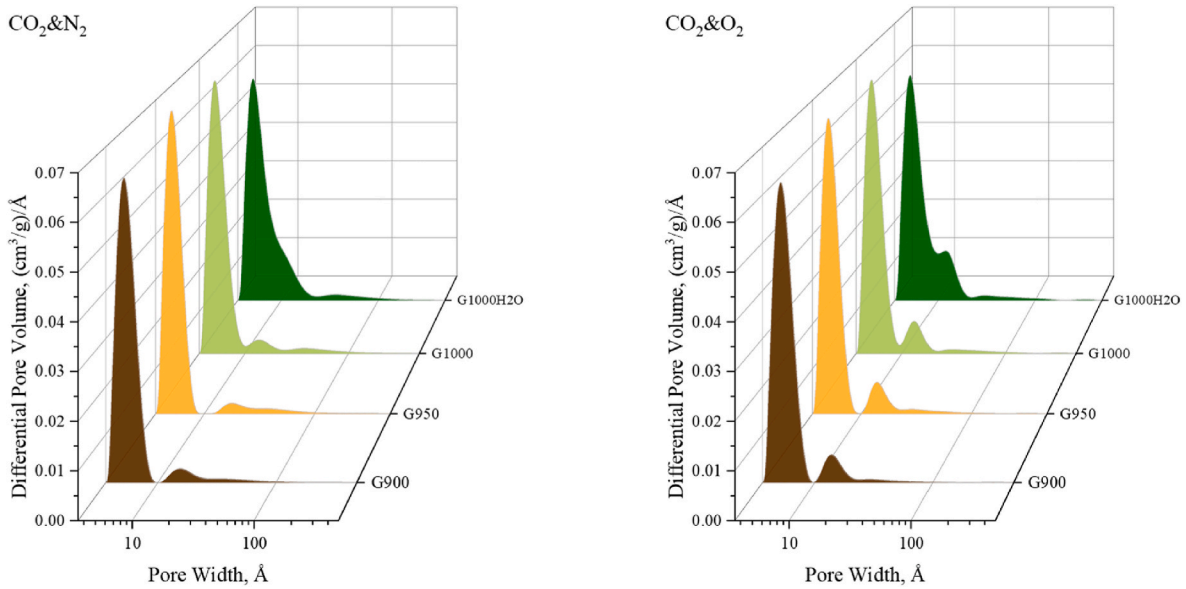


**Fig. 7.** The development of the gasification char PSD with the increase in gasification temperature (G900 to G1000) and the addition of steam (G1000 to G1000H2O).

e., supermicropores, was indicated by both $CO_2$ & $N_2$ and $CO_2$ & $O_2$ models (Fig. 6a). They also gave similar total pore volume, although the $CO_2$ & $O_2$ calculations attributed it to narrower pores, compared with $CO_2$ & $N_2$ (Fig. 6b). Thus, total surface area of gasification chars calculated with $CO_2$ & $O_2$ model was slightly higher than $CO_2$ & $N_2$ (Table 3). It is noticeable that both dual models gave significantly higher surface area, compared with the specific surface area calculated from the $N_2$ isotherm using the BET method.

### 3.3. Char activation during gasification step

In all four experiments, the pyrolysis was carried under the same conditions, and thus the pyrolytic chars, sampled after the first stage of biomass conversion, had similar pore distribution. The pyrolytic char transformation into the gasification char, i.e., the second conversion step, was performed at different temperatures and in the absence/presence of steam. Hence, four gasification chars with different degree of activation and carbon burn-off were obtained. As presented in Fig. 7, the increase in the gasification temperature slightly increased porosity of the char but did not affect the shape of the pore size distribution. On the other hand, the addition of steam resulted in a significant pore enlargement – the peak of ultramicropores decreased and widened towards the supermicropore region.

During the second step of the biomass conversion, the volatiles released during the pyrolysis undergo partial oxidation, while the pyrolytic char is gasified with the created gases. The syngas produced in the two-stage gasifier contained CO, $CO_2$, and $H_2$ – typically around 20 vol% of each. Water vapour from the inherent feedstock moisture was also present. Increased temperature of the gases passing through the char bed enhanced the pore volume from 0.140 $cm^3/g$ to 220–280 $cm^3/g$. The positive effect of the gasification temperature on pore development was observed, however, the most drastic changes occurred when steam was added to the process. The 100 °C increase in the reaction temperature increased the total pore volume by 25 %, while the addition of steam (1:5 water/feedstock ratio) enhanced it by another 30 %.

In the experiments without steam addition, the main char gasification agent is $CO_2$ from the partial oxidation of volatiles. Thus, the relatively small impact of the gasification temperature on char activation could result from a poor sensitivity of the $CO_2$ gasification kinetics to the increase in the reaction temperature. Another important aspect is the design of the two-stage gasifier. Changing gasification temperature affects mainly the gas-phase reactions in the upper part of the reactor (Fig. 1). Char particles that fall through this hot gas zone accumulate at the bottom, forming the char bed that maintains temperature in the range of 750–800 °C regardless of the gasification conditions. In other words, in this reactor, gasification temperature regulation aims at syngas composition adjustment, and it does not directly affect the heterogenous char-gas reactions. Thus, a strong impact of a reactor design on the correlation between process parameters and product characteristics should be always considered. For example, the construction of the gasifier used in this study resulted in the decreased sensitivity of the char pore formation to the gasification temperature.

The comparison of the gas adsorption models shows similar trend in the pore development examined with the $CO_2$ & $N_2$ and the $CO_2$ & $O_2$ combinations – the steam addition was required to widen the gasification char pores. Noticeably, even the char prepared under the severe gasification conditions (G1000H2O) had a highly microporous structure. As these pores are more accessible to $O_2$ molecules, the $CO_2$ & $O_2$ dual 2D-NLDFT model seems a suitable solution for char investigation at all stages of its formation, i.e., the pyrolysis followed by the thermal activation.

## 4. Conclusions

In this paper, we propose an approachable way to evaluate pore size distribution (PSD) of the ultramicroporous materials such as pyrogenic carbons. The dual 2D-NLDFT model for heterogenous carbons applied to two adsorption isotherms, $CO_2$ at 273 K and $O_2$ at 77 K, provided detailed and consistent PSDs for pyrolytic and gasification chars.

Good fit was obtained for the extremely ultramicroporous chars as well as the more opened structures. Using $O_2$ as the probe molecule allowed collecting the isotherms for the pyrolytic char, for which a negligible adsorption of $N_2$ was observed. Meanwhile, for the more activated chars, the analysis time was significantly shortened (almost 3 times for some samples), when $N_2$ was substituted with $O_2$.

Analysing the char from the semi-pilot scale gasifier confirmed the dependence of the char structure on the process parameters, but also suggested a strong impact of the reactor design. In the studied case, char porosity was not significantly affected by the gasification temperature, likely due to the short residence time of the char particles in the hot gas zone and the stabilized temperature of the forming char bed. Hence, it can be foreseen that each modification or scale-up of the gasification set

up will require a re-evaluation of char properties, calling for the quick and easy method for char structure monitoring.

The proposed approach seems to be a time-efficient method that can be performed without the need for advanced measurements, such as collecting the low pressure ($p/p_0$ from $10^{-7}$ to $10^{-3}$) part of the $N_2$ isotherm. Thus, it should be suitable as a day-to-day diagnostic tool for the pyrogenic char structure evaluation.

## CRediT authorship contribution statement

**Agnieszka Korus:** Writing – original draft, Visualization, Project administration, Methodology, Investigation, Funding acquisition, Conceptualization. **Jacek Jagiello:** Writing – review & editing, Software, Resources, Methodology. **Claus Dalsgaard Jensen:** Investigation. **Zsuzsa Sárossy:** Investigation. **Giulia Ravenni:** Writing – review & editing. **Lidia Benedini:** Investigation.

## Declaration of competing interest

The authors declare that they have no known competing financial interests or personal relationships that could have appeared to influence the work reported in this paper.

## Data availability

Measurements and calculations for "Advantages of dual CO2 & O2 adsorption model for assessment of micropore development in biochar during two-stage gasification" (Original data) (Mendeley Data)

## Acknowledgements

The research leading to these results has received funding from the Norway Grants 2014–2021 via the National Center for Research and Development. (Project no. NOR/SGS/FlowChar/0062/2020-01, "Flow electrodes from biomass-derived char", acronym: FlowChar, Small Grant Scheme 2020 Call)

## Appendix A. Supplementary data

Supplementary data to this article can be found online at https://doi.org/10.1016/j.renene.2024.120293.

## References

[1] D. Woolf, J.E. Amonette, F.A. Street-Perrott, J. Lehmann, S. Joseph, Sustainable biochar to mitigate global climate change, Nat. Commun. 1 (2010) 56, https://doi.org/10.1038/ncomms1053.
[2] J. Lehmann, S. Joseph, Biochar for Environmental Management: Science, Technology and Implementation, Routledge, 2015.
[3] D. Xu, L. Yang, K. Ding, Y. Zhang, W. Gao, Y. Huang, et al., Mini-review on char catalysts for tar reforming during biomass gasification: the importance of char structure, Energy Fuel. 34 (2020) 1219–1229, https://doi.org/10.1021/acs.energyfuels.9b03725.
[4] Q. Hu, J. Jung, D. Chen, K. Leong, S. Song, F. Li, et al., Biochar industry to circular economy, Sci. Total Environ. 757 (2021) 143820, https://doi.org/10.1016/J.SCITOTENV.2020.143820.
[5] J. Yuan, Y. Wen, D.D. Dionysiou, V.K. Sharma, X. Ma, Biochar as a novel carbon-negative electron source and mediator: electron exchange capacity (EEC) and environmentally persistent free radicals (EPFRs): a review, Chem Eng J 429 (2022) 132313, https://doi.org/10.1016/J.CEJ.2021.132313.
[6] A.M. Dehkhoda, N. Ellis, E. Gyenge, Effect of activated biochar porous structure on the capacitive deionization of NaCl and ZnCl2 solutions, Microporous Mesoporous Mater. 224 (2016) 217–228, https://doi.org/10.1016/j.micromeso.2015.11.041.
[7] W.J. Liu, H. Jiang, H.Q. Yu, Emerging applications of biochar-based materials for energy storage and conversion, Energy Environ. Sci. 12 (2019) 1751–1779, https://doi.org/10.1039/C9EE00206E.
[8] J. Lim, Y.U. Shin, S. Hong, Enhanced capacitive deionization using a biochar-integrated novel flow-electrode, Desalination 528 (2022) 115636, https://doi.org/10.1016/J.DESAL.2022.115636.
[9] X. Yuan, Y. Shen, P.A. Withana, O. Mašek, C.S.K. Lin, S. You, et al., Thermochemical upcycling of food waste into engineered biochar for energy and environmental applications: a critical review, Chem Eng J 469 (2023) 143783, https://doi.org/10.1016/J.CEJ.2023.143783.
[10] G.S. Ghodake, S.K. Shinde, A.A. Kadam, R.G. Saratale, G.D. Saratale, M. Kumar, et al., Review on biomass feedstocks, pyrolysis mechanism and physicochemical properties of biochar: state-of-the-art framework to speed up vision of circular bioeconomy, J. Clean. Prod. 297 (2021) 126645, https://doi.org/10.1016/J.JCLEPRO.2021.126645.
[11] K. Weber, P. Quicker, Properties of biochar, Fuel 217 (2018) 240–261, https://doi.org/10.1016/j.fuel.2017.12.054.
[12] F. Stoeckli, E. Daguerre, A. Guillot, Development of micropore volumes and widths during physical activation of various precursors, Carbon N Y 37 (1999) 2075–2077, https://doi.org/10.1016/S0008-6223(99)00220-1.
[13] Y. Liu, M. Paskevicius, M.V. Sofianos, G. Parkinson, S. Wang, C.Z. Li, A SAXS study of the pore structure evolution in biochar during gasification in H2O, CO2 and H2O/CO2, Fuel 292 (2021) 120384, https://doi.org/10.1016/j.fuel.2021.120384.
[14] Y. Bai, P. Lv, X. Yang, M. Gao, S. Zhu, L. Yan, et al., Gasification of coal char in H2O/CO2 atmospheres: evolution of surface morphology and pore structure, Fuel 218 (2018) 236–246, https://doi.org/10.1016/J.FUEL.2017.11.105.
[15] J.C. Maya, R. Macías, C.A. Gómez, F. Chejne, On the evolution of pore microstructure during coal char activation with steam/CO2 mixtures, Carbon N Y 158 (2020) 121–130, https://doi.org/10.1016/j.carbon.2019.11.088.
[16] P. Maziarka, C. Wurzer, P.J. Arauzo, A. Dieguez-Alonso, O. Mašek, F. Ronsse, Do you BET on routine? The reliability of N2 physisorption for the quantitative assessment of biochar's surface area, Chem Eng J 418 (2021) 129234, https://doi.org/10.1016/J.CEJ.2021.129234.
[17] Matthias Thommes, K. Katsumi, V. Na, P. Oj, Francisco R-R, Jean R, et al., Physisorption of gases, with special reference to the evaluation of surface area and pore size distribution (IUPAC Technical Report), Pure Appl. Chem. 87 (2015) 1051, https://doi.org/10.1515/pac-2014-1117.
[18] L. Leng, Q. Xiong, L. Yang, H.H. Li, Y. Zhou, W. Zhang, et al., An overview on engineering the surface area and porosity of biochar 763 (2021).
[19] J. Jagiello, C. Ania, J.B. Parra, C. Cook, Dual gas analysis of microporous carbons using 2D-NLDFT heterogeneous surface model and combined adsorption data of N2 and CO2, Carbon N Y 91 (2015) 330–337, https://doi.org/10.1016/J.CARBON.2015.05.004.
[20] L.S. Blankenship, J. Jagiello, R. Mokaya, Confirmation of pore formation mechanisms in biochars and activated carbons by dual isotherm analysis, Mater Adv (2022), https://doi.org/10.1039/D2MA00141A.
[21] J. Garrido, A. Linares-solano, J.M. Martìn-Martìnez, M. Molina-Sabio, F. Rodrìguez-Reinoso, R. Torregrosa, Use of nitrogen vs. carbon dioxide in the characterization of activated carbons, Langmuir 3 (2002) 76–81, https://doi.org/10.1021/LA00073A013.
[22] H. McLaughlin, F. Shields, J. Jagiello, G. Thiele, Analytical Options for Biochar Adsorption and Surface Area, North Am. Biochar Conf. Sonoma, CA, 2012.
[23] J. Jagiello, J. Kenvin, Consistency of carbon nanopore characteristics derived from adsorption of simple gases and 2D-NLDFT models. Advantages of using adsorption isotherms of oxygen (O2) at 77 K, J. Colloid Interface Sci. 542 (2019) 151–158, https://doi.org/10.1016/J.JCIS.2019.01.116.
[24] A. Beda, C. Vaulot, C. Matei Ghimbeu, Hard carbon porosity revealed by the adsorption of multiple gas probe molecules (N2, Ar, CO2, O2 and H2), J. Mater. Chem. A 9 (2021) 937–943, https://doi.org/10.1039/D0TA10088A.
[25] J. Jagiello, J. Kenvin, C.O. Ania, J.B. Parra, A. Celzard, V. Fierro, Exploiting the adsorption of simple gases O2 and H2 with minimal quadrupole moments for the dual gas characterization of nanoporous carbons using 2D-NLDFT models, Carbon N Y 160 (2020) 164–175, https://doi.org/10.1016/J.CARBON.2020.01.013.
[26] J. Jagiello, J.P. Olivier, 2D-NLDFT adsorption models for carbon slit-shaped pores with surface energetical heterogeneity and geometrical corrugation, Carbon N Y 55 (2013) 70–80, https://doi.org/10.1016/J.CARBON.2012.12.011.
[27] C. Nygaard, Gasification of Sewage Sludge in a Two-Stage Gasifier, Technical University of Denmark, Lyngby, 2015.
[28] J. Jagiello, J.P. Olivier, Carbon slit pore model incorporating surface energetical heterogeneity and geometrical corrugation, Adsorpt 19 (2013 192 2013) 777–783, https://doi.org/10.1007/S10450-013-9517-4.
[29] J. Jagiełło, Stable numerical solution of the adsorption integral equation using Splines, Langmuir 10 (2002) 2778–2785, https://doi.org/10.1021/LA00020A045.
[30] J. Jagiello, J. Kenvin, A. Celzard, V. Fierro, Enhanced resolution of ultra micropore size determination of biochars and activated carbons by dual gas analysis using N2 and CO2 with 2D-NLDFT adsorption models, Carbon N Y 144 (2019) 206–215, https://doi.org/10.1016/j.carbon.2018.12.028.
[31] G. Ravenni, O.H. Elhami, J. Ahrenfeldt, U.B. Henriksen, Y. Neubauer, Adsorption and decomposition of tar model compounds over the surface of gasification char and active carbon within the temperature range 250–800 °C, Appl. Energy 241 (2019) 139–151, https://doi.org/10.1016/J.APENERGY.2019.03.032.
[32] N. Sun, J. Qiu, B. Xu, Understanding of sodium storage mechanism in hard carbons: ongoing development under debate, Adv. Energy Mater. 12 (2022) 2200715, https://doi.org/10.1002/AENM.202200715.